

01 Nov 2000

## Detection of Solid Pigment in Dermatoscopy Images using Texture Analysis

Murali Anantha

William V. Stoecker

*Missouri University of Science and Technology*

Randy Hays Moss

*Missouri University of Science and Technology, rhm@mst.edu*

Follow this and additional works at: [https://scholarsmine.mst.edu/chem\\_facwork](https://scholarsmine.mst.edu/chem_facwork)

 Part of the [Chemistry Commons](#), and the [Electrical and Computer Engineering Commons](#)

---

### Recommended Citation

M. Anantha et al., "Detection of Solid Pigment in Dermatoscopy Images using Texture Analysis," *Skin Research and Technology*, vol. 6, no. 4, pp. 193-198, John Wiley & Sons, Nov 2000.

The definitive version is available at <https://doi.org/10.1034/j.1600-0846.2000.006004193.x>

This Article - Journal is brought to you for free and open access by Scholars' Mine. It has been accepted for inclusion in Chemistry Faculty Research & Creative Works by an authorized administrator of Scholars' Mine. This work is protected by U. S. Copyright Law. Unauthorized use including reproduction for redistribution requires the permission of the copyright holder. For more information, please contact [scholarsmine@mst.edu](mailto:scholarsmine@mst.edu).

## Detection of solid pigment in dermatoscopy images using texture analysis

Anantha Murali<sup>1</sup>, William V. Stoecker<sup>2</sup>, and Randy H. Moss<sup>3</sup>

<sup>1</sup>D2 Technologies, Santa Barbara, CA

<sup>2</sup>Stoecker & Associates, Rolla, and Dermatology M173, University of Missouri Health Sciences Center, MO

<sup>3</sup>Department of Electrical and Computer Engineering, University of Missouri-Rolla, Rolla, MO, USA

### Abstract

**Background/aims**—Epiluminescence microscopy (ELM), also known as dermoscopy or dermatoscopy, is a non-invasive, in vivo technique, that permits visualization of features of pigmented melanocytic neoplasms that are not discernable by examination with the naked eye. ELM offers a completely new range of visual features. One such feature is the solid pigment, also called the blotchy pigment or dark structureless area. Our goal was to automatically detect this feature and determine whether its presence is useful in distinguishing benign from malignant pigmented lesions.

**Methods**—Here, a texture-based algorithm is developed for the detection of solid pigment. The factors  $d$  and  $a$  used in calculating neighboring gray level dependence matrix (NGLDM) numbers were chosen as optimum by experimentation. The algorithms are tested on a set of 37 images. A new index is presented for separation of benign and malignant lesions, based on the presence of solid pigment in the periphery.

**Results**—The NGLDM large number emphasis N2 was satisfactory for the detection of the solid pigment. Nine lesions had solid pigment detected, and among our 37 lesions, no melanoma lacked solid pigment. The index for separation of benign and malignant lesions was applied to the nine lesions. We were able to separate the benign lesions with solid pigment from the malignant lesions with the exception of only one lesion, a Spitz nevus that mimicked a malignant melanoma.

**Conclusion**—Texture methods may be useful in detecting important dermatoscopy features in digitized images and a new index may be useful in separating benign from malignant lesions. Testing on a larger set of lesions is needed before further conclusions can be made.

### Keywords

solid pigment; dermatoscopy; melanoma; image analysis; texture

---

Malignant melanoma is a lethal form of skin cancer that has claimed many lives in recent years. Over the past decade the number of people affected by this disease has doubled in most parts of the world. In the United States alone, around 44,200 new cases of melanoma are estimated in 1999 (1). The number of deaths estimated from this deadly disease was

around 7000 in 1999 (1). Since melanoma can be cured if detected early, early detection is extremely important for the survival of the patient.

Epiluminescence microscopy (ELM), also known as skin-surface microscopy, or dermatoscopy or dermoscopy, was described in 1921 (2) and later in 1987 (3). It is a non-invasive tool to improve the early diagnosis of malignant melanoma. Initially, it was designed to be used with complex microscopic equipment. However, ELM now is used in a general clinical setting with an inexpensive hand-held otoscope-like unit (4). ELM combines oil immersion with standard magnifying optics and incident surface lighting to permit in vivo visualization of features of pigmented melanocytic neoplasms that are not discernable by examination with the naked eye. ELM offers a completely new range of visual features, such as the pigment network, solid pigment, radial streaming, globules and blue/gray veil, to aid the diagnostic process.

The procedure consists of first applying alcohol or mineral oil to the pigmented skin lesion. A transparent material is then pressed against the lesion after which it is examined under tangential illumination with magnification. This technique reduces the reflected light from the irregular surface of the stratum corneum and thus makes the epidermis more transparent so that structures at the dermal-epidermal junction and upper dermis may be visualized (4). The use of ELM can increase experts' diagnostic accuracy for pigmented lesions, assisting in clinically differentiating melanoma from its benign simulators (3, 5).

Texture analysis is the attempt to quantify texture notions, such as “fine”, “rough” and “irregular”, and identify, measure, and utilize the differences between them (6). A point has no texture; only a region can have a texture. The most prominent feature that discriminates between textured and non-textured images is the coarseness, or the size of textural primitives. Coarseness of an image is not absolute but depends on the scale at which the image is processed. Reducing the size of the image makes a textured image seem smoother, while magnifying the image brings forward the rough structure of the surface. Textural features and texture analysis methods can be loosely divided into two categories – statistical and structural. Statistical methods define texture in terms of local gray-level statistics that are constant or slowly varying over a textured region. Different textures can be discriminated by comparing the statistics computed over different sub-regions. Structural texture models try to determine the primitives of which the texture is composed. While statistical features measure gray-value variations in an image neighborhood, structural features explicitly characterize properties of textural primitives, such as their size and shape (7). In clinical dermatology images, one study noted superior texture discrimination with statistical methods in identifying smoothness (6). This paper develops a statistical technique for detecting solid pigment.

Solid pigment is one of the many features that occur in dermoscopic images. It refers to regions on the lesions in which the pigment is so dominant that the pigment network, also a feature in dermoscopic images, becomes indiscernible. Solid pigment is important because it provides a feature that is helpful in differentiating malignant from benign lesions. A rotation invariant approach, developed by Sun & Wee (8), defines a matrix called the neighboring gray-level dependence matrix that summarizes the relationship between pixels and all their neighbors. This method considers the relationship between a pixel element and all its neighbors at one time instead of one direction at a time, and thus eliminates angular dependency. However different matrices are still needed for different values of distances. Sun & Wee also suggested five texture attributes, namely, small number emphasis, large number emphasis, number nonuniformity, second moment and entropy.

## Neighboring Gray-level Dependence Matrix

The neighboring gray level dependence matrix (NGLDM) records the frequency that the given gray level has a specified number of neighbors with the same gray level. Therefore, the coordinates of the two-dimensional NGLDM are the gray-level value and the number of neighbors. Let  $k$  be the gray-level coordinate, such that  $0 \leq k \leq K$ , and  $s$  be the number-of-neighbors coordinates, such that  $0 \leq s \leq S$ . Here  $K$  is the possible set of gray levels in the image  $I$ , and  $S$  is the total number of possible neighbors within the distance  $d$ . Image  $I(i, j)$  is an  $M \times M$  gray-scale image, such that  $0 \leq i, j \leq M-1$ . Let  $d > 0$  be an integer that represents the maximum distance between the pixel and its neighbors.  $d=1$  indicates the immediate  $3 \times 3$  area,  $d=2$  is the surrounding  $5 \times 5$  area and so on. Note that if  $d=1$ , then  $S=8$ , and if  $d=2$ ,  $S=24$ , i.e.,  $S=4d^2+4d$ . Let  $a \geq 0$  be an integer that specifies the maximum difference between the pixel gray level that is considered equal; that is, when searching for the neighbors with the same gray level, accept those pixels that have a value within  $\pm a$  intensity-level difference from the intensity level of the center pixel. Mathematically, the NGLDM,  $Q(k, s)$ , is defined by this equation:

$$Q(k, s) = \# \{ (i, j) \mid I(i, j) = k \text{ and } \# \{ (m, n) \mid \rho((i, j), (m, n)) \leq d \text{ and } |I(i, j) - I(m, n)| \leq a \} = s \}$$

and

$$|I(i, j) - I(m, n)| \leq a \quad (1)$$

where  $\#$  denotes the number of elements in the set,  $\rho((i, j), (m, n))$  indicates the distance between the elements  $(i, j)$  and  $(m, n)$ , and  $d$  and  $a$  are positive integers that can be selected according to the coarseness of the image under consideration (8).

The  $Q$  matrix contains the texture information of an image. The texture coarseness or fineness of an image can be interpreted as the distribution of the entities in the  $Q$  matrix. To compute the  $Q$  matrix from the image  $I$ , calculate  $s$  for each point  $(i, j)$  by counting the points in the neighborhood of  $(i, j)$  whose value is within  $\pm a$  of  $I(i, j)=k$ ; increment  $Q(k, s)$ . Note that if each pixel is to have the same number of neighbors, the pixels at the edge of the image must be ignored – that is, constrain  $(i, j)$  such that  $d \leq i, j \leq M-1-d$  (8).

Texture attribute statistics can be computed from the  $Q$  matrix (8). One measure that was used for the analysis is large number emphasis:

$$N2 = \frac{\sum_{k=1}^K \sum_{s=1}^S [s^2 Q(K, s)]}{\sum_{k=1}^K \sum_{s=1}^S Q(K, s)} \quad (2)$$

where  $K$  is the number of gray-level values in the image and  $S$  is the number of NGLDM numbers.

In this analysis, the large number emphasis  $N2$  was used for classification, as this attribute gave a clear threshold for identifying the solid pigment.

## Dermatoscopy Images

Thirty-seven dermatoscopy images of malignant melanomas, nevocellular nevi and dysplastic nevi were digitized at a resolution of 512×480, in full 24-bit color. Images were acquired with a Heine dermaphot camera and Fujichrome film.

The software program Dullrazor (9) was applied to all images to remove hair. For each of the 37 tumor images, for each 64×64 block, 49 per image, a dermatologist (WVS) scored the block for pigment network presence or absence.

## Methods

In malignant melanoma, solid pigment often occurs in patches, solid at one edge or irregularly scattered around the periphery. The NGLDM approach is used for the identification of solid pigment in images. The algorithm was tested on a set of 37 images. In the first level of processing, the color image is converted into a luminance image defined as follows:

$$\text{Lum Image} = 0.29R + 0.59G + 0.11B \quad (3)$$

where  $R$ ,  $G$ ,  $B$  are the red, green and blue color components. The image is divided into 64×64-pixel blocks. Each of these blocks is given as input to the algorithm, and the NGLDM numbers are calculated for every block using equations 1 and 2. After experimenting with various values of  $d$  and  $a$ , the values of  $d=5$  and  $a=4$  were chosen for the analysis as the optimum parameters. The NGLDM numbers are stored in a data file. The data files have both the image number and the NGLDM numbers corresponding to that image. Pagadala's algorithm (4) is used to determine the borders for the tumor images, which are then stored as run-length-coded files. Only blocks that are fully inside the tumor are selected for analysis. This is done so that the edge effects that occur, considering the partial blocks, are avoided. The decision as to the presence of solid pigment is a two-stage process. The first stage involves setting a threshold on the NGLDM N2 large number emphasis for each block. Blocks whose NGLDM N2 numbers are below the threshold are considered for the color filtering stage. Solid pigment tends to contain a lot of red color component. The condition enforced was that the average red color in a block be less than level 80 and the average of the red and green color component in that block be less than level 150. All color levels lie between 0 and 255. This is used to decide the existence of solid pigment. The steps for the detection of solid pigment are summarized by a flow chart in Fig. 1.

A normalized pigment centroid distance measure is also calculated for the solid pigment. This measure uses the square of the distance of the pigment block from the centroid normalized by similar measures for the best-fit ellipse as shown below in equation 13. The centroid of all the full blocks in the tumor was found. Then the distance between the blocks detected as solid pigment and the centroid of the tumor is calculated. The zero-, first- and the second-order moments are calculated, from which the central moments are calculated and, in turn, the major and the minor axis of the best-fitting ellipse is found. The expressions for all the measures are defined below for an  $M \times M$  image  $I$ . The zero, first- and second-order moments are:

$$m_{00} = \sum_{i=1}^M \sum_{j=1}^M I(i, j) \quad (4)$$

$$m01 = \sum_{i=1}^M \sum_{j=1}^M i * I(i, j) \quad (5a)$$

$$m10 = \sum_{i=1}^M \sum_{j=1}^M j * I(i, j) \quad (5b)$$

$$m02 = \sum_{i=1}^M \sum_{j=1}^M i^2 * I(i, j) \quad (6a)$$

$$m11 = \sum_{i=1}^M \sum_{j=1}^M i * j * I(i, j) \quad (6b)$$

$$m20 = \sum_{i=1}^M \sum_{j=1}^M j^2 * I(i, j) \quad (6c)$$

where  $m00$  is the zero-order moment;  $m01$ ,  $m10$  are the first-order moments; and  $m02$ ,  $m11$ ,  $m20$  are the second-order moments. The central moments are:

$$\mu00 = m00 \quad (7)$$

$$\mu20 = m20 - (m10^2 / m00) \quad (8)$$

$$\mu02 = m02 - (m01^2 / m00) \quad (9)$$

$$\mu11 = m11 - (m10 * m01 / m00) \quad (10)$$

where  $\mu00$  is the zero-order central moment;  $\mu01$ ,  $\mu10$  are the first-order central moments; and  $\mu02$ ,  $\mu11$ ,  $\mu20$  are the second-order central moments.

The major and minor axes are:

$$a = \sqrt{\frac{\mu20 + \mu02 + \sqrt{(\mu20 - \mu02)^2 + (4\mu11)^2}}{\mu00/2}} \quad (11)$$

$$b = \sqrt{\frac{\mu_{20} + \mu_{02} - \sqrt{(\mu_{20} - \mu_{02})^2 + (4\mu_{11})^2}}{\mu_{00}/2}} \quad (12)$$

where  $a$  is the length of the major axis of the best fitting ellipse and  $b$  is the length of the minor axis of the best fitting ellipse.

The normalized pigment centroid distance measure for block  $i$  is:

$$\frac{(x_i - x_c)^2 + (y_i - y_c)^2}{(a^2 + b^2)} \quad (13)$$

where  $x_i$  and  $y_i$  are the coordinates of the center of the block classified by the algorithm as solid pigment, and  $x_c$  and  $y_c$  are the coordinates of the centroid of all the complete blocks in the tumor. The results are averaged over all the blocks detected as solid pigment blocks to create the normalized pigment centroid distance measure.

## Results

Results of the solid-pigment-finder algorithm are shown in Figs. 2–5. The results of the application of the solid-pigment-detection algorithm to the images were evaluated by a dermatologist (WVS) and are shown in Table 1. Figure 6 shows the plot of the normalized pigment centroid distance measure against image number. Only nine of the thirty-seven images were found to have solid pigment and hence are the only ones shown in Fig. 6. It can be seen from the figure that images 106d, 112d and 1227d have distance measures greater than 0.3. These have been diagnosed as malignant. This stresses the hypothesis that images with solid pigment and whose distance measure is high are typically malignant. An exception to this hypothesis was seen in image 1239d, which was diagnosed as a Spitz nevus – a mimic of malignant melanoma. In general, it was observed that the solid-pigment finder detected most of the solid pigment in the images. In some cases the partial blocks caused a problem in determining the presence of the solid pigment.

## Conclusions

The NGLDM large number emphasis N2 was satisfactory for the detection of the solid pigment. The index for separation of benign and malignant lesions was able to separate the benign lesions with solid pigment from the malignant lesions with the exception of only one lesion, a Spitz nevus that mimicked a malignant melanoma. Texture methods may be useful in detecting important dermatoscopy features in digitized images, and a new index may be useful in separating benign from malignant lesions.

With the present computing power and technology, steps are being taken towards automating the detection and diagnosis of malignant melanoma using digital dermatoscopy. Solid pigment is one feature that can aid the diagnostic process. Conclusions about the usefulness of the peripheral pigment index are limited by the small number of lesions tested. Future work will include a greater number of lesions for testing as well as implementation of a peripheral patchy solid pigmentation index to detect irregular peripheral distribution of solid pigment that may be more indicative of melanoma than peripheral pigment alone.

## Acknowledgments

This work was supported in part by NIH SBIR grant 1R43 CA- 60294. The authors wish to thank Armand Cognetta, M.D., Matthew Fleming, M.D., and Wilhelm Stolz, M.D., for supplying dermatoscopy images. Kathy Whyte helped significantly as system administrator.

## References

1. Landis SH, Murray T, Bolden S, Wingo PA. Estimated new cases of cancer by site. *Cancer Statistics*. 1999; 49:12.
2. Saphier J. Die Dermatoskopie. I. Mitteilung. *Arch f Dermat und Syph*. 1921; 128:1–19.
3. Steiner A, Pehamberger H, Wolff K. Improvement of diagnostic accuracy in pigmented skin lesions by epiluminescent light microscopy. *Anticancer Res*. 1987; 7:433–434. [PubMed: 3631897]
4. Pagadala, P. Master of Science in Electrical Engineering Thesis. University of Missouri–Rolla; 1998. Tumor border detection in epiluminiscence microscopy images.
5. Binder M, Schwarz M, Winkler A, et al. Epiluminescence microscopy: a useful tool for the diagnosis of pigmented skin lesions for formally trained dermatologists. *Arch Dermatol*. 1995; 13:286–291. [PubMed: 7887657]
6. Stoecker WV, Li WW, Moss RH. Texture in skin images: comparison of three methods to determine smoothness. *Comput Med Imaging Graph*. 1992; 10:179–190. [PubMed: 1623493]
7. Harris, DE. Doctorate in Electrical Engineering Dissertation. University of Missouri–Rolla; 1994. Texture analysis of skin cancer images.
8. Sun C, Wee WG. Neighboring gray level dependence matrix for texture classification. *Comput Vis Graph Image Process*. 1983; 23:341–352.
9. Lee T, Ng V, Gallagher R, Coldman A, McLean D. DullRazor: a software approach to hair removal. *Comp Biol Med*. 1997; 27:533–543.



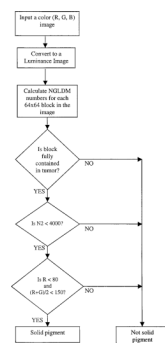


**Fig. 1.**  
Flow chart illustrating steps for detecting solid pigment.

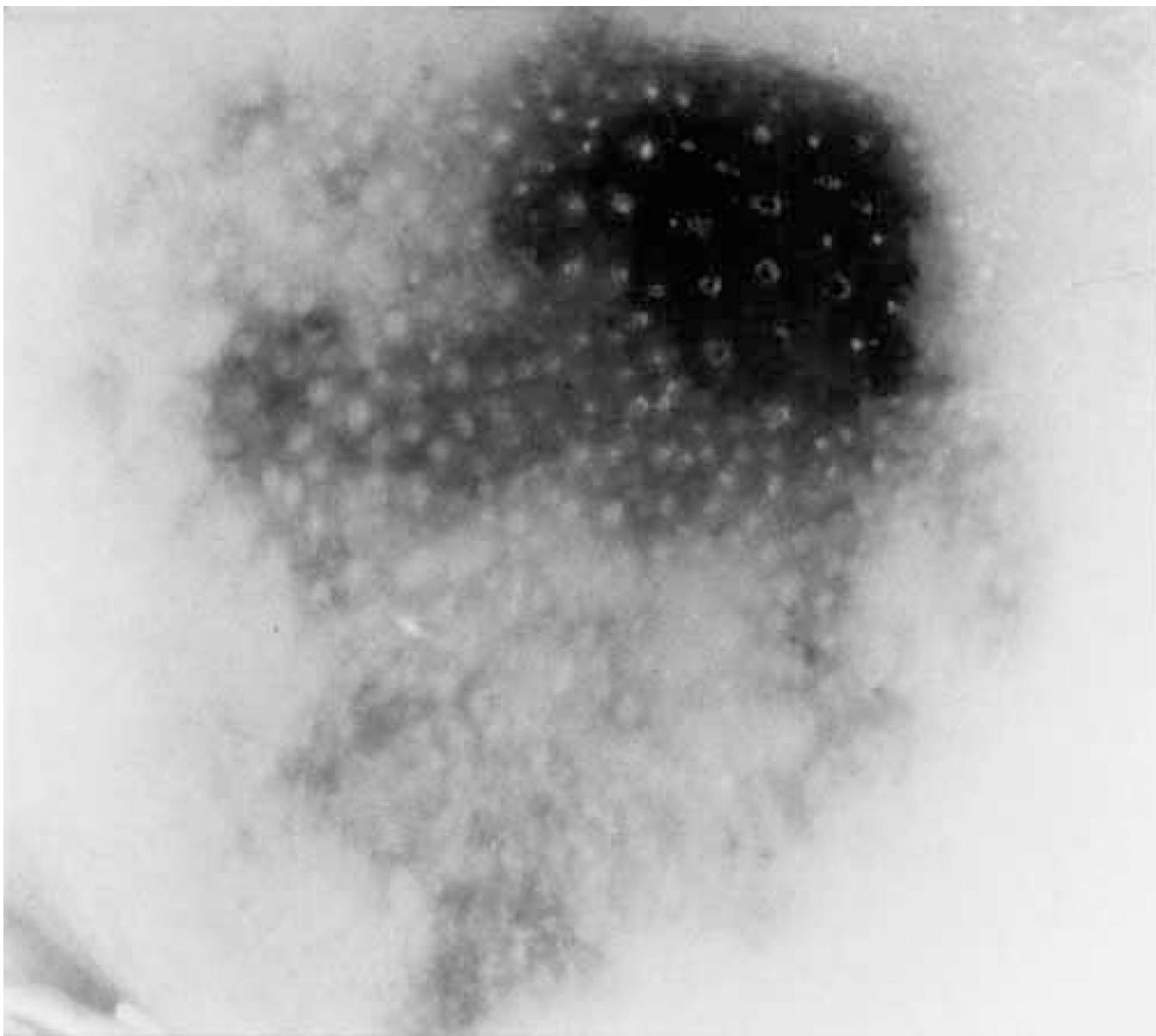


**Fig. 2.**  
Melanoma with solid pigment.

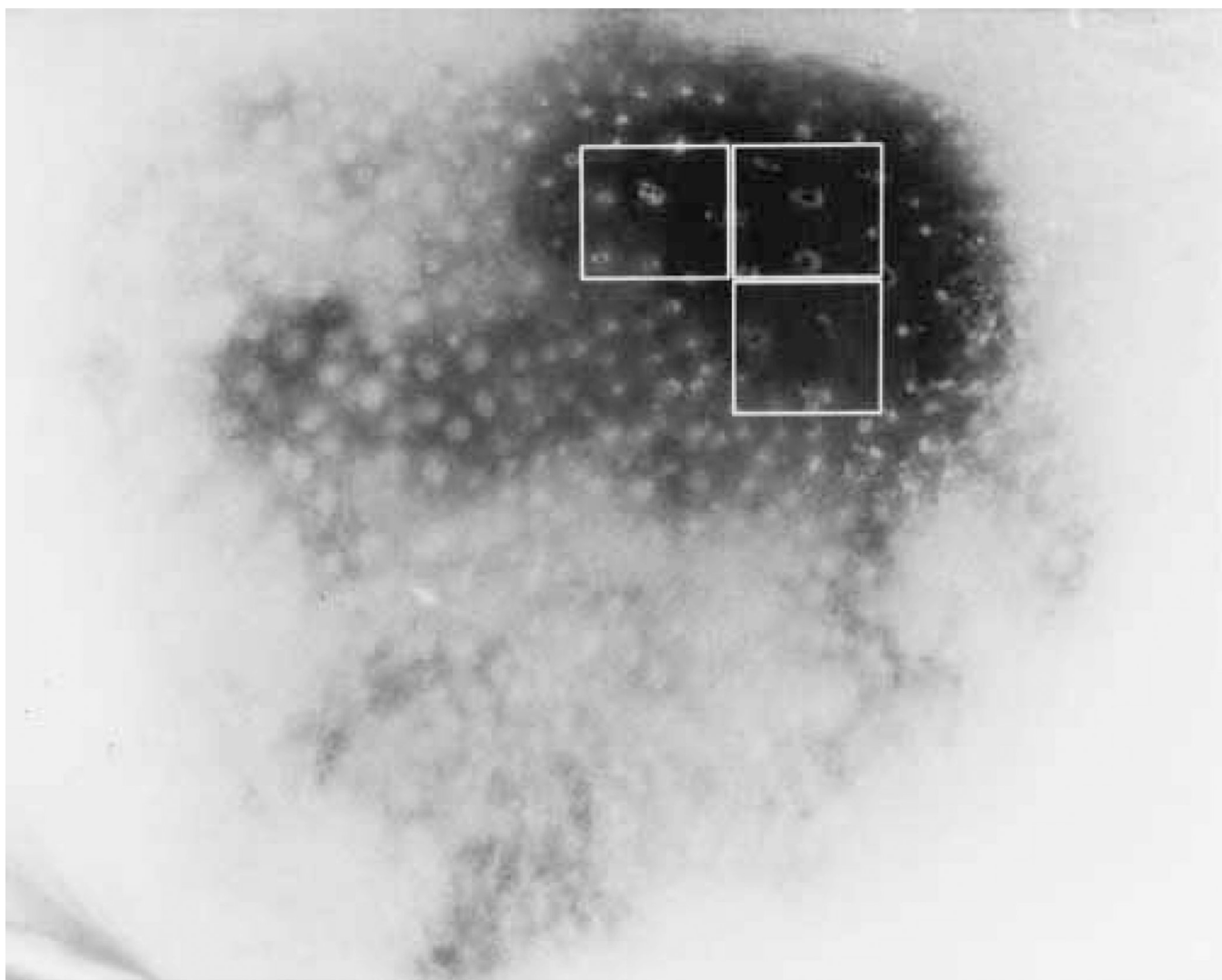


**Fig. 3.**  
Melanoma with solid pigment detected. Note that only complete blocks within the lesion area are found.

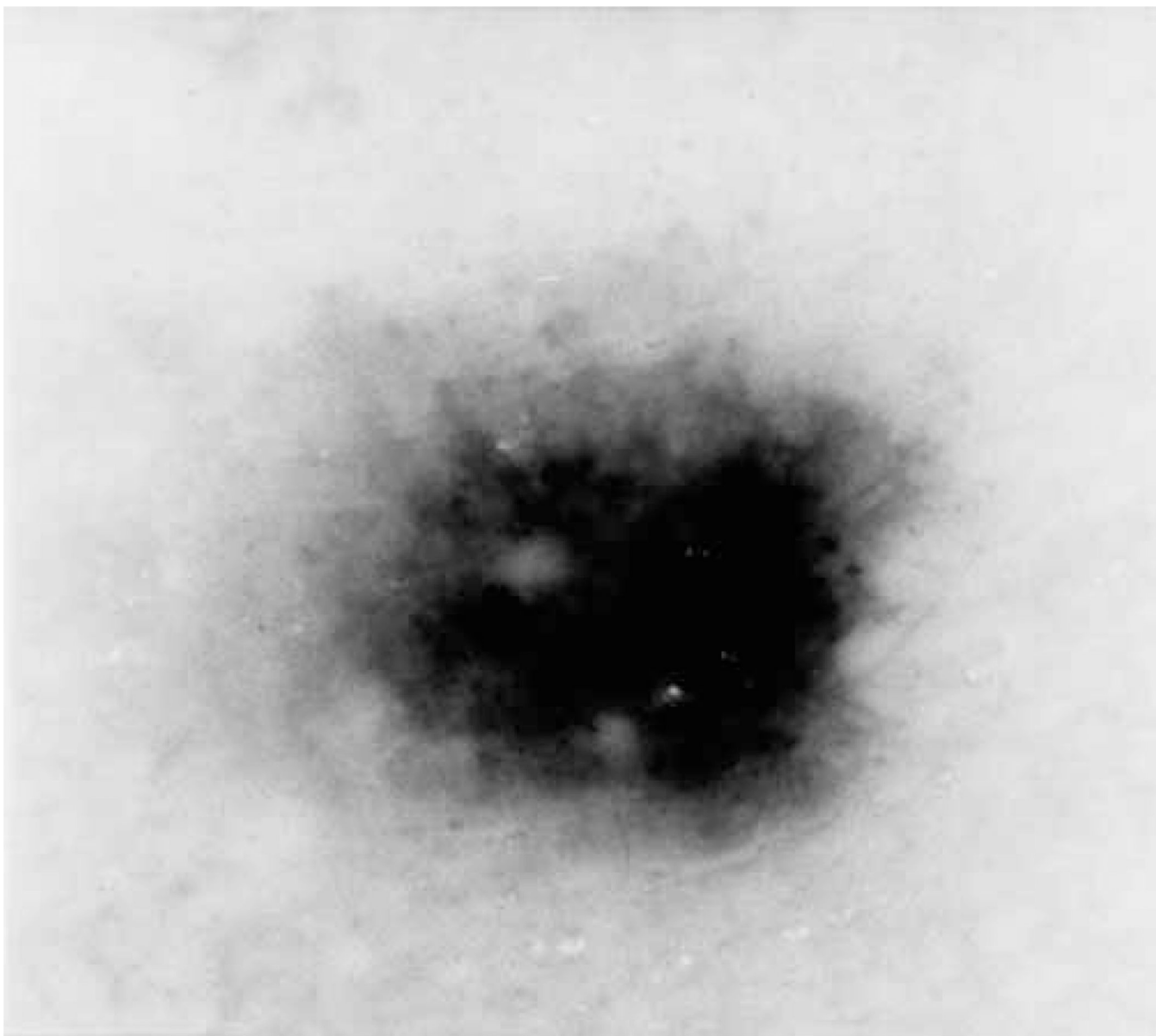


**Fig. 4.**  
Benign nevus.

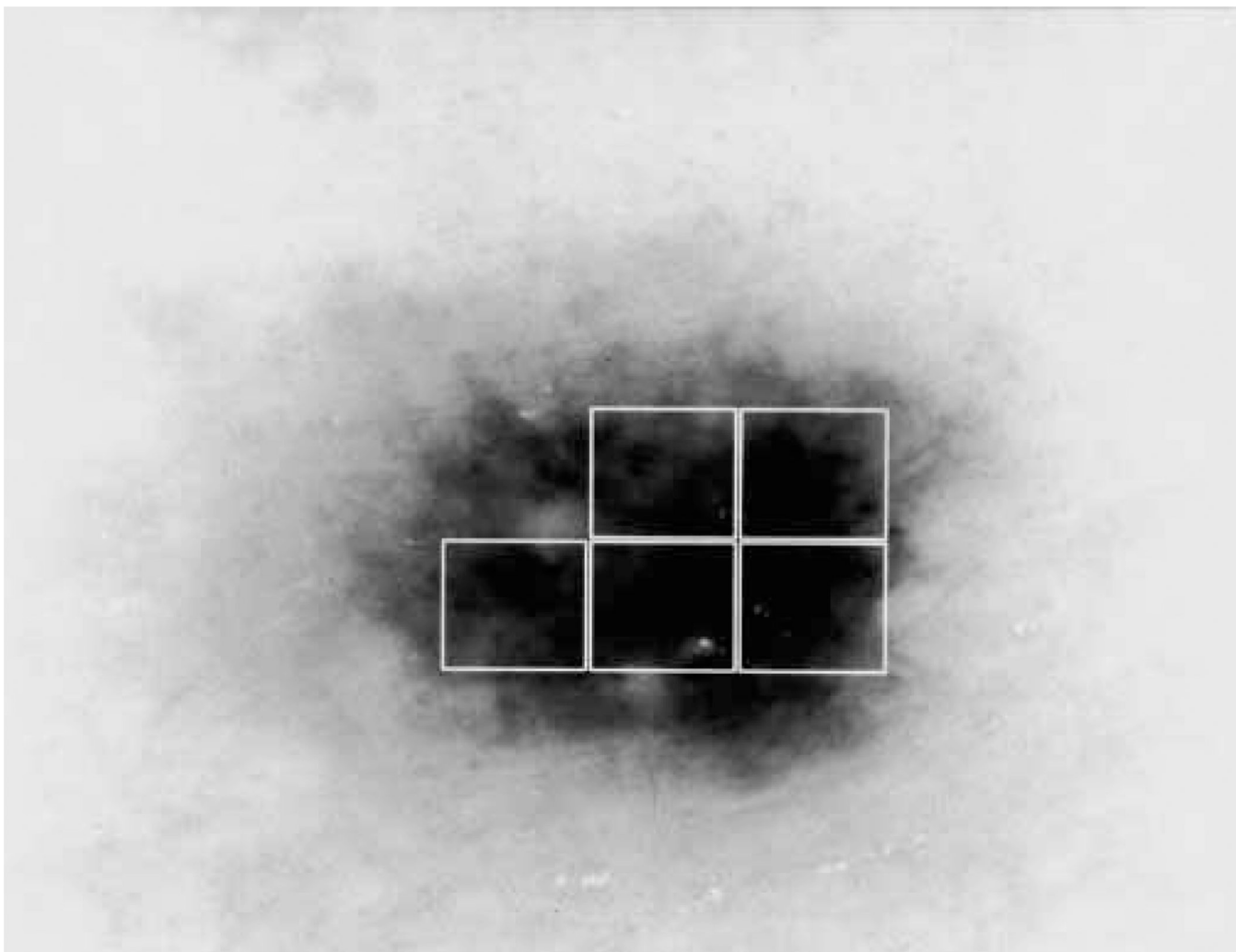


**Fig. 5.**  
Benign nevus with solid pigment detected. Note that the left upper block lacks enough solid pigment to allow detection.

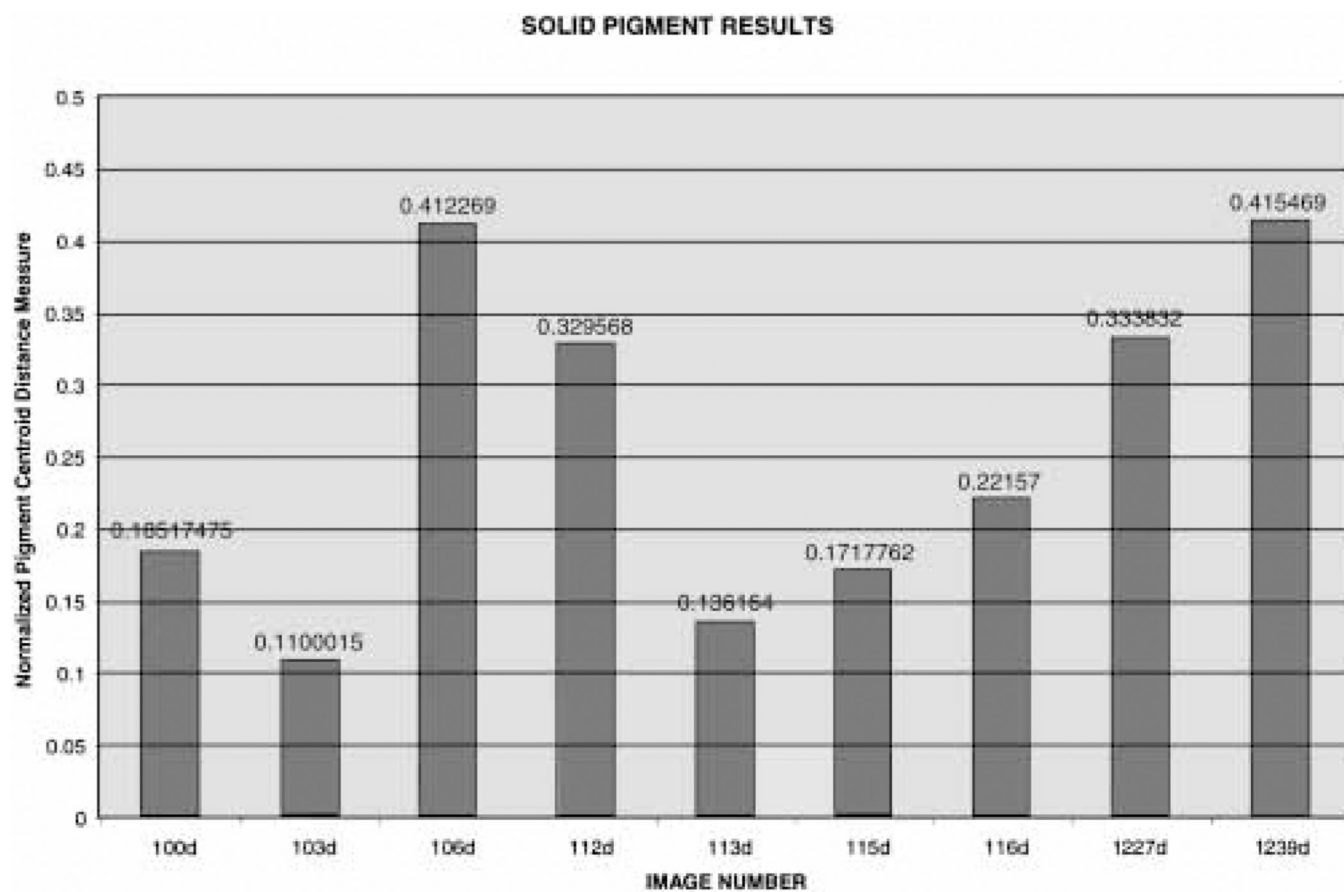


**Fig. 6.** Normalized pigment centroid distance measure for various images. 106d and 112d are malignant. 1239d is a Spitz nevus for which excision is recommended.

**TABLE 1**

Results of the solid-pigment finder on various images

Image number	Results of solid-pigment finder Missed/Extra*	Remarks
100d	0/0	**
101d	0/0	Partial solid blocks in the center, benign
102d	0/0	Benign
103d	0/1	Left lower block is partial, benign
104d	0/0	Dysplastic nevus, benign
105d	0/0	Benign
106d	0/0	Melanoma (Breslow 1.05 mm)
107d	0/0	Lentigo maligna
108d	0/0	Lentigo maligna
109d	0/0	Benign
110d	0/0	Benign
111d	0/0	Benign
112d	0/1	Melanoma, (Breslow 0.55 mm)**
113d	0/0	Benign
114d	0/0	Benign
115d	0/0	Partial solid pigment in left upper corner block, benign
116d	0/0	Galaxy-like appearance, benign**
117d	0/0	Benign
1223d	0/0	Dark image, melanoma
1224d	0/0	Melanoma
1225d	0/0	Melanoma
1226d	0/0	Melanoma
1227d	1/0	Melanoma, radial streaming, white streaks
1228d	0/0	Melanoma
1229d	0/0	Melanoma
1230d	0/0	Melanoma
1231d	0/0	Melanoma
1232d	0/0	Benign
1233d	0/0	Benign
1234d	0/0	Melanoma
1235d	0/0	Benign
1236d	0/0	Benign
1237d	0/0	Benign
1238d	0/0	Benign
1239d	0/0	Spitz nevus <sup>†</sup> , **
1240d	0/0	Benign
1241d	0/0	Benign

\* Refers to the number of solid-pigment blocks found by the dermatologist as missed by the algorithm and the number found by the algorithm and said by the dermatologist to be not solid pigment, respectively, i.e., the dermatologist provided the gold standard.

\*\* Border does not include any full solid-pigment blocks.

† A Spitz nevus resembles a melanoma clinically and excision is generally recommended.